Science Advances
AAAS

advances.sciencemag.org/cgi/content/full/4/10/eaat9039/DC1

Supplementary Materials for

Mass spectrometry imaging of the in situ drug release from nanocarriers

Jinjuan Xue, Huihui Liu, Suming Chen*, Caiqiao Xiong*, Lingpeng Zhan, Jie Sun, Zongxiu Nie*

*Corresponding author. Email: schen145@jhmi.edu (S.C.); xiongcq@iccas.ac.cn (C.X.); znie@iccas.ac.cn (Z.N.)

Published 31 October 2018, *Sci. Adv.* **4**, eaat9039 (2018)
DOI: 10.1126/sciadv.aat9039

This PDF file includes:

Supplementary Materials and Methods

LA-PEG synthesis

Lipoic acid conjugated PEG (LA-PEG) was synthesized as previous report (*19*). Briefly, 500 mg mPEG-NH_2 and 45 mg lipoic acid was mixed in 2 mL dichloromethane, then 10 mg of N,N'-dicyclohexylcarbodiimide as dehydrating reagent and 6 μL triethylamine as catalyst were added into the above mixture. Then the dehydration reaction was carried out at room temperature for 24 h. After that dichloromethane were blown to dry under a nitrogen flow, then 10 mL deionized water was added into the dried solid. The water insoluble solid was removed by filtration. The pH of the filter was adjusted to 8 with sodium bicarbonate (0.1 M) and filter was extracted by dichloromethane for three times. Then dichloromethane were evaporated to dryness by a rotary evaporator (Hei-VAP Advantage, Heidolph Instruments GmbH & Co.KG, Germany) at 30 ℃. Finally, the product was dissolved in 10 mL deionized water and lyophilized. The final product was stored at -20 ℃ for future use.

Drug release

Drug release experiment was carried out with a dialysis bag immersed in different pH value PBS solution. And at different time points, the PBS solution outside the dialysis bag was take out to measure their UV-Vis adsorption at 490 nm, then the drug release percentage can be calculated.

Cell lines

The mouse hepatoma cell line H22 was purchased from Department of Laboratory Animal Science, Peking University Health Center. 4T1 cell line was obtained from Research Center for Eco-Environmental Sciences, Chinese Academy of Sciences.

Cell cultured experiments

4T1 Cells were cultured in RPMI1640 medium (containing 100 U/mL penicillin and 100 mg/ml streptomycin) with 10% fetal bovine serum at 37 ℃ under 5% CO_2.

Animal Tumor Model

Subcutaneously implanted 4T1 and H22 tumor model were established by subcutaneously injecting 4T1 or H22 cells (1×10^7 cells dispersed in 200 μL PBS) into the armpit of the female Balb/c mice or male Kunming mice.

Orthotopic H22 tumor model was established as the following steps:

- The mice were anesthetized by intraperitoneal injection of 10% chloral hydrate (3 mg/g)
- After the mice were in deep anesthesia, fix the limbs of the mice onto an operating table.
- Sterilize the abdomen with 75% alcohol.
- Expose the liver by midline incision.
- Directly intrahepatic inject 1×10^6 H22 cells (dispersed in 50 μL PBS) into the left lobe of the liver with a micro syringe.
- Compress the insertion point gently to avoid the reflux of tumor cells.
- Close the abdomen with 5-0 silk suture.

H&E staining procedures for cryostat section

After the cryostat sections were mounted onto the adhesion microscope slides, immediately dip the slides into the cool acetone for 20 s to complete the fixation of the sections. Then the H&E staining procedures are as following:

- Hydration: dip the slides into tap water for 1 second.
- Hematoxylin staining: 8 minutes
- Washing: wash with running water for several times
- Differentiation: dip into 0.5% HCl-ethanol for 1 second
- Washing: wash with running water for several times
- Dip into aqueous ammonia for 1 second
- Washing: wash with running water first and then wash with deionized water
- Eosin staining: 20 seconds
- Washing: wash with deionized water
- Transparent treatment: use gradient alcohol and xylene for transparent treatment of dyed slices. 70% ethanol (2 minutes) - 80% ethanol (2 minutes) - 90% ethanol (2 minutes) - anhydrous ethanol (2 minutes) - xylene I (5 minutes) - xylene II (5 minutes)
- Neutral gum sealing dyed slices

Quantification of MoS_2 nanosheets in organs by imaging mass spectrometry

Quantification of MoS_2 nanosheets in organs was following our previous reported tissue homogenate imaging mass spectrometry method (*15*). The detailed protocol was as following:

- Establish the calibration curves of each organ.

The organs of normal mice were harvested and weighed to prepare tissue homogenate. The weighed organs were transferred into centrifuge tubes. For better lysis the tissue with a homogenizer, 1% sodium dodecyl sulfate (SDS) solution was added to the weighed organs (3 μL/mg tissue) to lyses cells so that endocytic MoS_2 nanosheets could be released. The lysis homogenate was then heated at 70 ℃ for 2 h to get a clear solution. Then the tissue homogenate was spiked with a series different concentration of MoS_2 nanosheets for each organ. The spiked tissue homogenate (about 100 μL) was added into a 1 mL disposable syringe (the end was cut open) and dipped into liquid nitrogen for 30 s to freeze the homogenate into a cylindrical solid. Then the syringe with homogenate solid was place in a -20 ℃ freezer for at least half an hour. After that, the solid was pushed out of the syringe and the solid was sectioned into 25 μm thickness slices in a Leica CM1950 cryostat (Leica Biosystems, Nussloch, Germany). Three parallel slices for each concentration of MoS_2 nanosheets homogenate was prepared. Then the slices ware thaw-mounted onto the conductive side of an ITO-coated glass slide (Bruker Daltonics, Bremen, Germany) and dried for at least 30 min in a vacuum desiccator before mass spectrometry analysis. Mass spectrometry imaging was performed with 200 μm laser resolution in each slice. After imaging, the average ion intensity of $[MoS_2O_2]^-$ (choosing the strongest isotope peak *m/z* = 193.8 as representative) could be read out with FlexImaging 4.0 software (Bruker Daltonics) for each slice. Then plotted the average ion intensity to the MoS_2 nanosheets concentration, the calibration curve could be obtained. Calibration curves for lung, spleen and liver are shown in fig. S17.

- Measuring the MoS_2 nanosheets concentration in the organs of MoS_2 nanosheets injected mice.

The preparation of tissue homogenate and cryostat section of each organ was carried out as the same protocol as above. For different dosing time the organs of three individual mice were carried out as parallel experiment. The parameters of mass spectrometry analysis of the injected mice need to be kept exactly same with calibration curve measurement. According to the average ion intensity of each organ slice and the calibration curve, the MoS_2 nanosheets concentration could be calculated. Since the individual differences of the size of the organ, we use percent injected dose (%ID) instead of concentration to quantify the MoS_2 nanosheets in organs. The calculation

between %ID and concentration of homogenate was as the following equation

$$ID\% = \frac{\left[MoS_2 nanosheets\right]_{lysate} \times V_{lysate}}{\left[MoS_2 nanosheets\right]_{injected} \times V_{injected}} \times 100\%$$

Quantification of Mo in organs by ICP-MS

In order to quantify the Mo in organs by ICP-MS, 100 μL of the homogenate of each MoS_2 nanosheets injected mice which was prepared in the previous procedure was added into a Teflon Crucible, then 4 mL concentrated HNO_3 was added to predigest the homogenate overnight. After predigested, 3 mL 30% H_2O_2 was added for further digestion open in air on a 150 ℃ hot plate until the residual liquid was about 1 mL, then added 2.5 mL aqua regia and continued to digest to the remaining liquid was about 0.5 mL. Finally, the left liquid was cooled down to room temperature and diluted to 5 mL with a diluted acid mixture solution (1% HCl and 2% HNO_3). At the mean time a blank sample (100 μL 1% SDS solution replaced the homogenate) was done with the same procedure. Before ICP MS quantification of the sample solution, an external calibration curve was obtained by testing the spiked series standard Mo solution (0.1 ppb, 1 ppb, 10 ppb, 100 ppb, 1000 ppb) on an Agilent 7700 series ICP-MS instrument. After calibration， the sample solution was tested and the Mo element amount could be obtained. Since Mo was a trace element in organism (*34*), three normal mice organ were also tested as control. The content of Mo element in tissue (μg/mg) measured by ICP was calculated as the following equation

$$\text{Content of Mo in tissue} = \frac{[\text{Mo}]_{\text{diluent}} \times \text{dilution ratio} \times \text{V}_{\text{lysate}}}{\text{tissue weight}}$$

To facilitate the comparison of the quantification results by LDI MSI and ICP MS, we convert percent injected dose (%ID) measured by LDI MSI into content of Mo in tissue measured by ICP MS via the following equation

$$\text{Content of Mo in tissue} = \frac{\left[MoS_2\ nanosheets\right] \times \text{V}_{\text{lysate}} \times \frac{Ar_{Mo}}{Mr_{MoS_2}}}{tissue\ weight}$$

Loading of doxorubicin onto CNTs

The received multi-walled carbon nanotubes were oxidized by refluxing with 5 M HNO_3 for 12 hours, then, neutralized by saturated Na_2CO_3 solution. After that, the solution was the dialyzed against de-ionized water through a dialysis membrane (MWCO 3500) for 48 h. Finally, oxidized carbon nanotube was obtained by lyophilization.

For drug loading, 10 mg oxidized carbon nanotubes were added into 50 mL saturated doxorubicin PBS solution (pH = 8), after sonication for 30 min, the solution was stirred at room temperature for 24 h to complete the drug loading process. After loading, the excess free DOX was removed by centrifugal filtration, and washed with PBS buffer for several times. The successful drug loading was proved by UV-Vis (fig. S14E)). Characterization of the CNTs and DOX-CNT by LDI MSI were shown in fig. S14B) and S14C).

For LDI MSI, DOX-CNT was intravenous injected to normal mice (5 mg/kg CNTs). The mice were sacrificed 24 h after the intravenous administration, tissues were harvested and dissected. The MSI results were shown in fig. S14F).

Loading of doxorubicin onto BP nanosheets

BP nanosheets were synthesized as previously reported (*35*). Briefly, 100 mg of the received black phosphorus powder was added into 10 mL deionized water, then the mixed solution was treated with tip sonication for 15 h (On/Off cycle: 60 s/15 s) in ice bath. After sonication the brown dispersion was centrifuged 1000 rpm for 10 min to get rid of the unexfoliated BP powders. Then the supernatant containing BP nanosheets was added to NH_2-PEG solution, sonicated for 1 h and stirred overnight to complete the modification the BP nanosheets with PEG to increase the solubility and biocompatibility in physiological conditions.

For drug loading, 10 mg PEG modified BP nanosheets were added into 50 mL saturated doxorubicin PBS solution (pH = 8), the solution was stirred at room temperature for 24 h to complete the drug loading process. After loading, the excess free DOX was removed by centrifugal filtration, and washed with PBS buffer for several times. The successful drug loading was proved by UV-Vis (fig. S15G). Characterization of the CNTs and DOX-BP by LDI MSI were shown in fig. S15B and S15E).

For LDI MSI, DOX-BP was intravenous injected to normal mice (5 mg/kg BP nanosheets). The mice were sacrificed 24 h after the intravenous administration, tissues were harvested and dissected. The MSI results were shown in fig. S15H).

Loading of doxorubicin onto gold nanoparticles

Chitosan-capped gold nanoparticles was synthesized by adding 49 mg of $HAuCl_4 \cdot 3H_2O$/mL into 100 mL boiling 0.05% chitosan solution (containing 1% acetic acid). When the color of the solution turned into ruby red, cool the solution down to room temperature. Then 14000 rpm centrifuged to remove excess chitosan. The chitosan-capped gold nanoparticles was stored at 4 ℃ in dark. For drug loading, 125 μg/mL of DOX-hydrochloride was added to each milliliter of chitosan-capped gold nanoparticles solution. Then mixture was shake overnight and then DOX was loaded on the gold nanoparticle surface based on the interaction of chitosan's ($–NH_2$) groups of DOX.

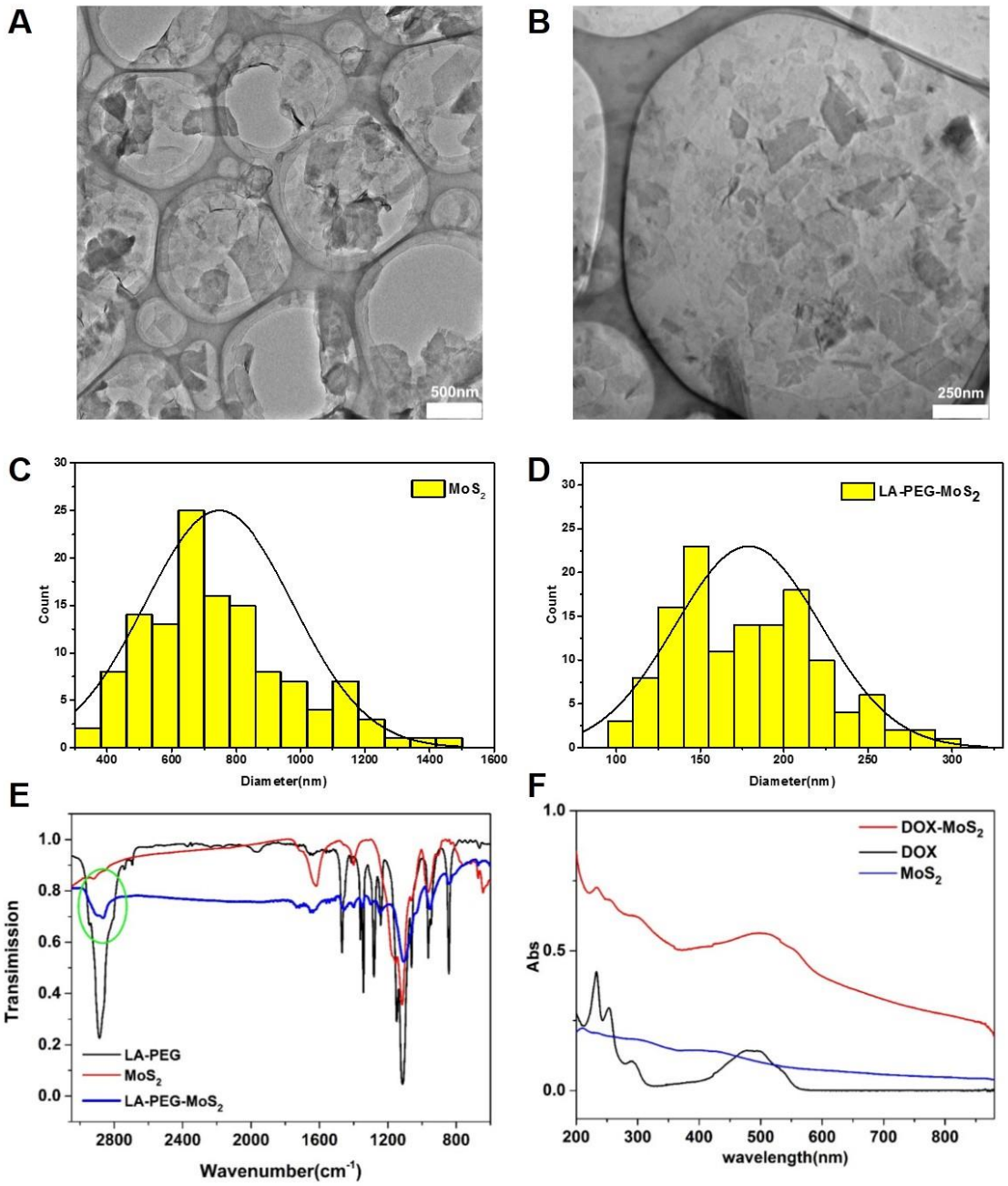

Fig. S1. Characterization of MoS_2 nanosheets. TEM image of bare MoS_2 nanosheets (**A**) and LA-PEG modified MoS_2 nanosheets (**B**). Lateral size distribution of bare MoS_2 nanosheets (**C**) and LA-PEG modified MoS_2 nanosheets (**D**). Spectroscopic characterization of MoS_2 nanosheets. (**E**) FT-IR spectra of LA-PEG (black line), MoS_2 nanosheets without LA-PEG modification (red line) and MoS_2 nanosheets with LA-PEG modification (blue line). The green circle indicates the IR adsorption band at about 2900 cm^{-1} belonged to C-H vibration in LA-PEG. (**F**) UV-vis adsorption spectra of bare MoS_2 nanosheets (blue line), DOX (black line) and DOX/PEG-MoS_2 nanosheets (red line). The strong UV absorption of MoS_2 nanosheets ($\varepsilon = 3.02\times10^6$ L • mol^{-1} cm^{-1} at 355 nm) facilitated the LDI process under the irradiation of laser of MALDI mass spectrometer.

A

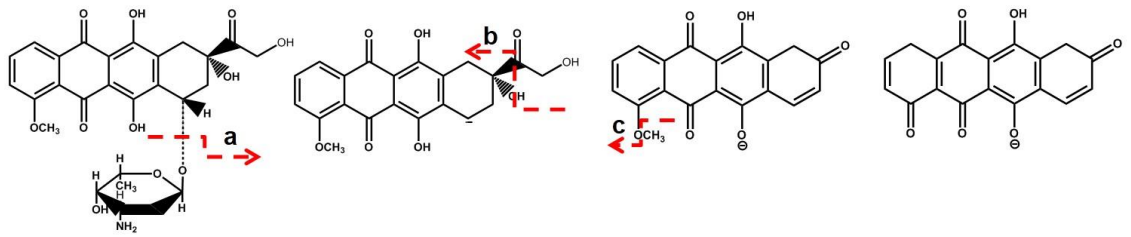

DOX: MW=543.5 a: m/z=396.1 b: m/z=335.0 c: m/z=321.0

B

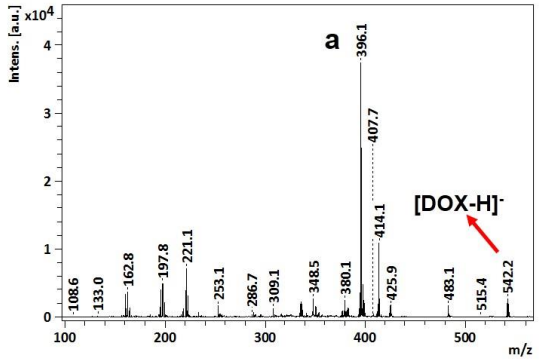

C

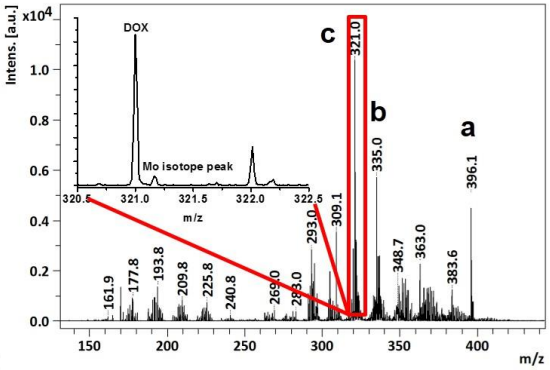

D

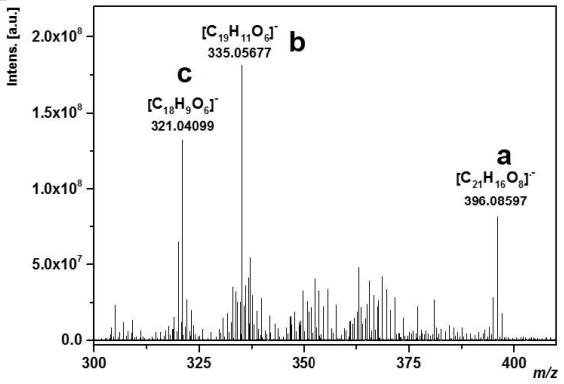

E

	Theoretical mass (Da)	Observed mass(Da)	Error (ppm)
a	396.08507	396.08597	-2.28
b	335.05611	335.05677	-1.96
c	321.04046	321.04099	-1.64

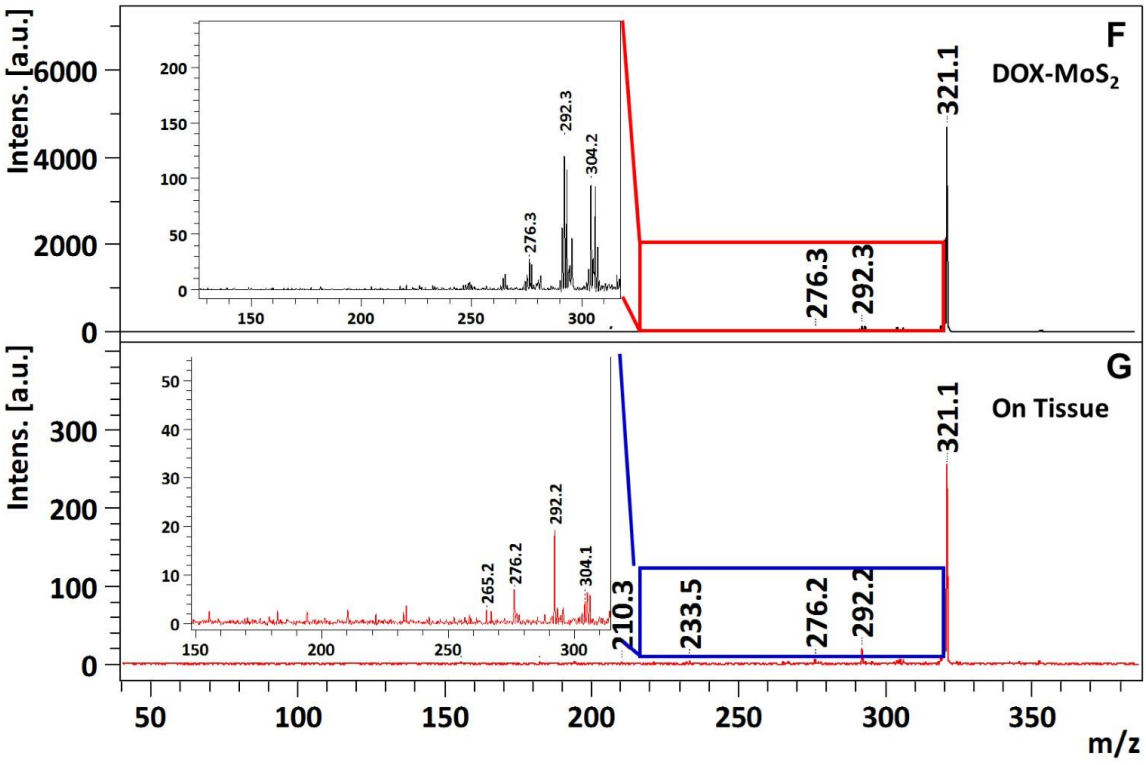

Fig. S2. Identification of DOX fingerprint mass peak. (**A**). In-source decay pathways of DOX. (**B**). MALDI-TOF mass spectra of pure DOX with N-(1-naphthyl) ethylenediamine dihydrochloride (NEDC) as matrix. (**C**). MALDI-TOF mass spectra of DOX with MoS_2 nanosheets as matrix, the inset showed the DOX fragment peak discriminated from the Mo isotope peak. (**D**). MALDI-FT-ICR high-resolution mass spectra to determine the DOX fragment. (**E**). Corresponding DOX fragment identification results by high-resolution MS. (**F**) MS/MS mass spectra of *m/z* = 321 obtained from DOX/PEG-MoS_2 nanosheets mixture spotted directly onto the MALDI target plate. (**G**) MS/MS mass spectra of *m/z* = 321 obtained from DOX/PEG-MoS_2 nanosheets injected mice tissue.

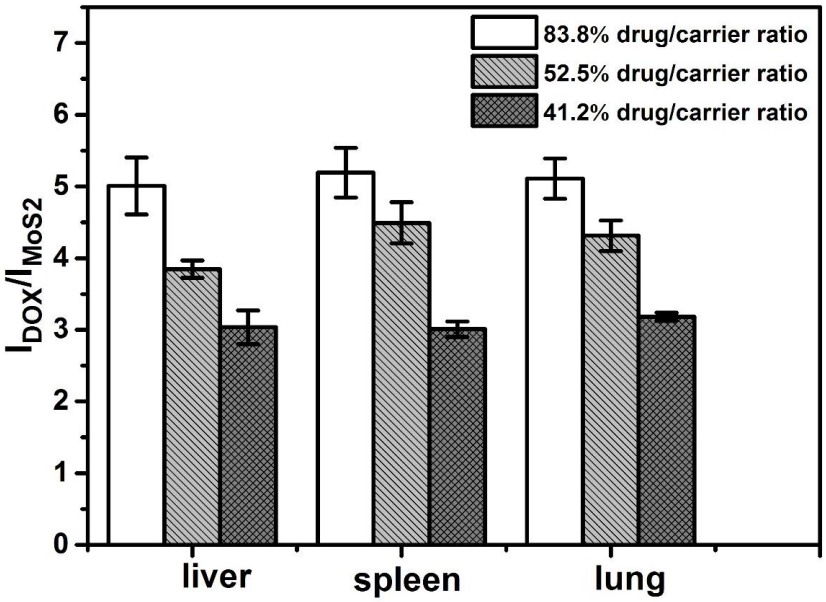

Fig. S3. Average ion intensity ratios of the DOX/PEG-MoS_2 with different loading ratios. DOX/PEG-MoS_2 are spiked in liver, spleen and lung tissue homogenates. Average ion intensity ratio of DOX fingerprint anions (*m/z* = 321.0) to MoS_2 nanosheets fingerprint anions (*m/z* = 193.8) (noted as: I_{DOX}/I_{MoS2}) in liver spleen and lung tissue homogenate spiked with DOX/PEG-MoS_2 nanosheets with gradient drug loading ratio.

Biodistribution of MoS_2 nanosheets revealed by LDI MSI

The demonstration of the time-variation biodistribution and retention in the biological systems is crucial for the development of the drug carriers. To evaluate the performance of MoS_2 nanosheets as nanocarriers, we first investigated the detailed biodistribution of bare MoS_2 nanosheets over the time to figure out the carrier circulation time and behavior. To get this through, we harvested the organs of the mice from different time points of intravenous injection of bare MoS_2 nanosheets.

No detectable ion signal was observed for any tissue obtained from control mice tissues (fig. S4), even when irradiated with the highest laser energy (~100 μJ) allowed by our experimental set-up. In contrast, the tissue samples derived from MoS_2-injected mice showed the unique MoS_2-derivative ions at the expected m/z values (fig. S4). This observation supports the expectation that these fingerprint anions could indeed be used to represent the existence of MoS_2 nanosheets in tissues. The LDI MSI images generated with the intensity of $[MoS_2O_2]^-$ anions (*m/z* = 193.8 is used as representative peak to generate the images throughout the experiments) were shown in fig. S5-S7. It can be inferred that MoS_2 nanosheets have a long circulation time in the blood stream. At short time points, e.g., 1 h and 5 h, MoS_2 nanosheets mainly enriched in lung, and a very small fraction distribution can be found in liver, spleen, almost none MS signal was detected in heart, kidney and brain. However, with the circulation time prolonging to 24 h or 48 h, stronger signal can be found in spleen and liver, still little signal was found in kidney, heart and brain. This can be explained by the fact that the large lateral size of MoS_2 nanosheets (750 ± 230 nm) might be hard to be cleared by glomerular filtration of kidney, and is difficult to break the blood barrier of the heart and brain. When the circulation time was increased to 15 days, the MS signal of MoS_2 nanosheets begins to decrease in all organs, this means MoS_2 nanosheets would be gradually cleared from the biosystem of mice with longer circulation time. Finally by the time of 30 days (the longest tracking time in our experiment) much more of the MoS_2 nanosheets were cleared, but still some lower intensity of MS signal were found in lung, spleen and liver. Such a long retention time in the reticuloendothelial system may be beneficial to extend the circulation time of payload drugs in the nanotherapeutics. The sub-organ distributions of MoS_2 nanosheets in spleen were also characterized (fig. S7). The LDI MS images clearly suggest that the nanosheets accumulated mostly in red pulp regions and especially the marginal zones, which is consistent with the observation of carbon nanomaterials in our previous work (S. Chen, et al. Nat. Nanotech. 2015, 10, 176). These results demonstrated the ability of the LDI MSI method to the biodistribution study of MoS_2 nanosheets in the tissues.

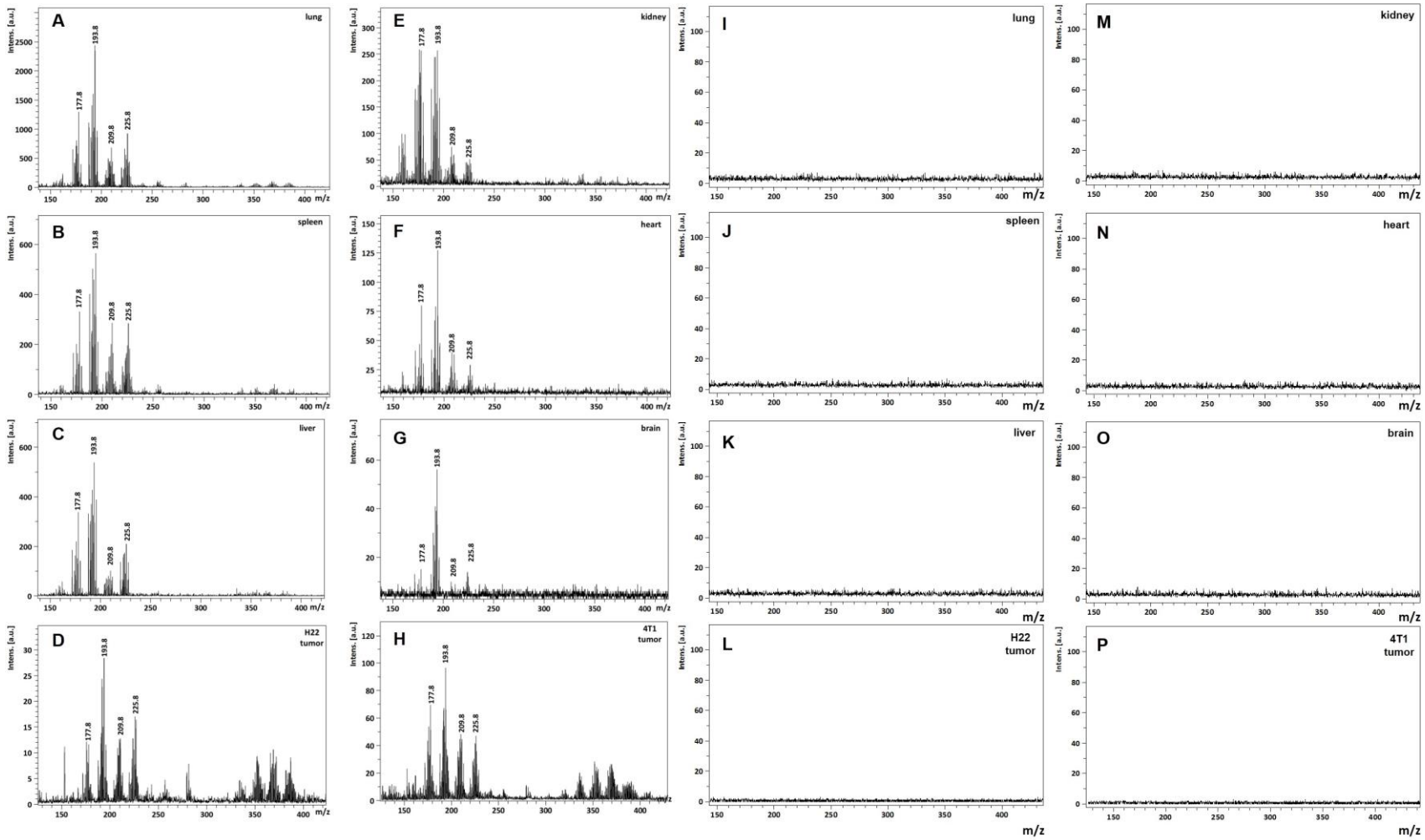

Fig. S4. Representative LDI MS spectra in mice tissues. Representative LDI mass spectra of bare MoS_2 nanosheets injected-mice tissue slices (**A** to **H**) and representative LDI mass spectra of mice tissue slices (**I** to **P**). Tissues are lung, spleen, liver, kidney, heart, brain, H22 tumor and 4T1 tumor.

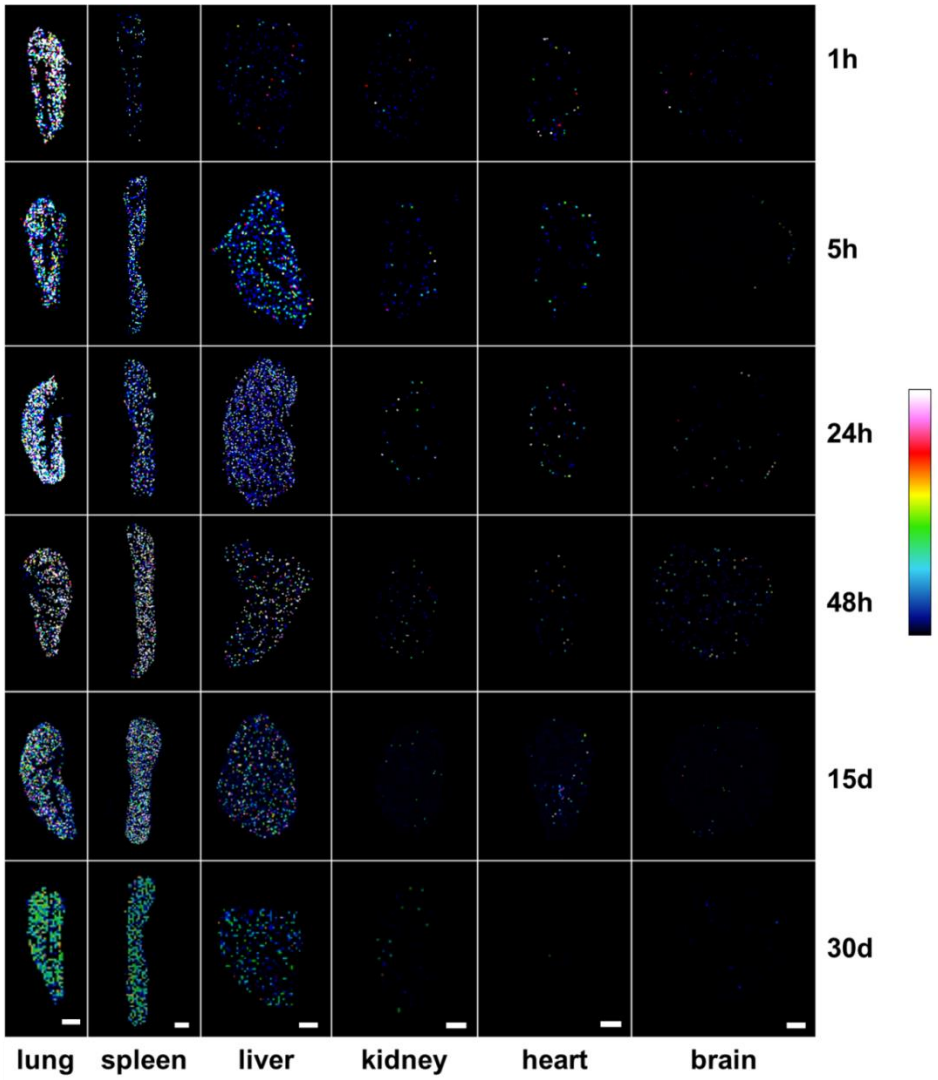

Fig. S5. LDI MSI images of tissues in normal mice. These images show the time-variation sub-organ distribution of bare MoS_2 nanosheets in lung, spleen, liver, kidney, heart and brain tissues. Three to five tissue sections of each organ for each of the experimental groups were obtained from MoS_2-injected mice and subjected to LDI MS imaging. Each group of images showed similar distributional patterns. Scale bar: 5 mm. The color bar on the right indicates the intensity increase from 0 to 100% from bottom to top. The concave region in the lung tissues is the trachea area.

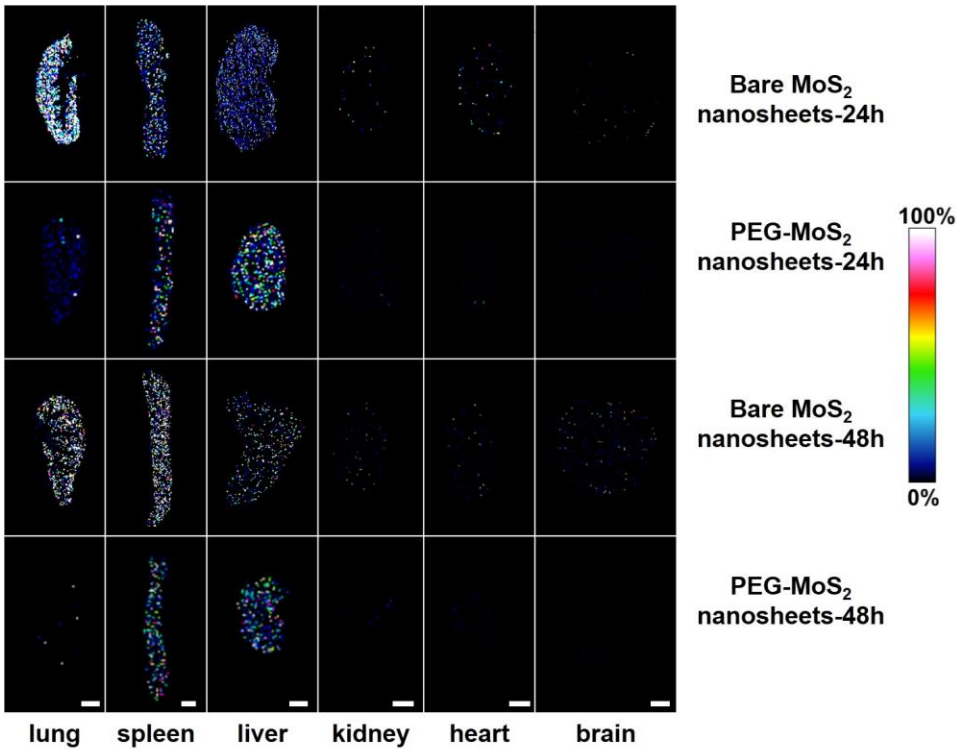

Fig. S6. LDI MSI images of tissues injected with bare and LA-PEG–modified MoS_2 nanosheets (PEG-MoS_2) in normal mice. These images show the sub-organ distribution of bare MoS_2 nanosheets and LA-PEG-modified MoS_2 nanosheets in lung, spleen, liver, kidney, heart and brain tissues after 24 h and 48 h injection. Three to five tissue sections of each organ for each of the experimental groups were obtained from MoS_2-injected or PEG-MoS_2-injected mice and subjected to LDI MS imaging. Each group of images showed similar distributional patterns. Scale bar: 5 mm. The color bar on the right indicates the intensity increase from 0 to 100% from bottom to top. The concave region in the lung tissues is the trachea area.

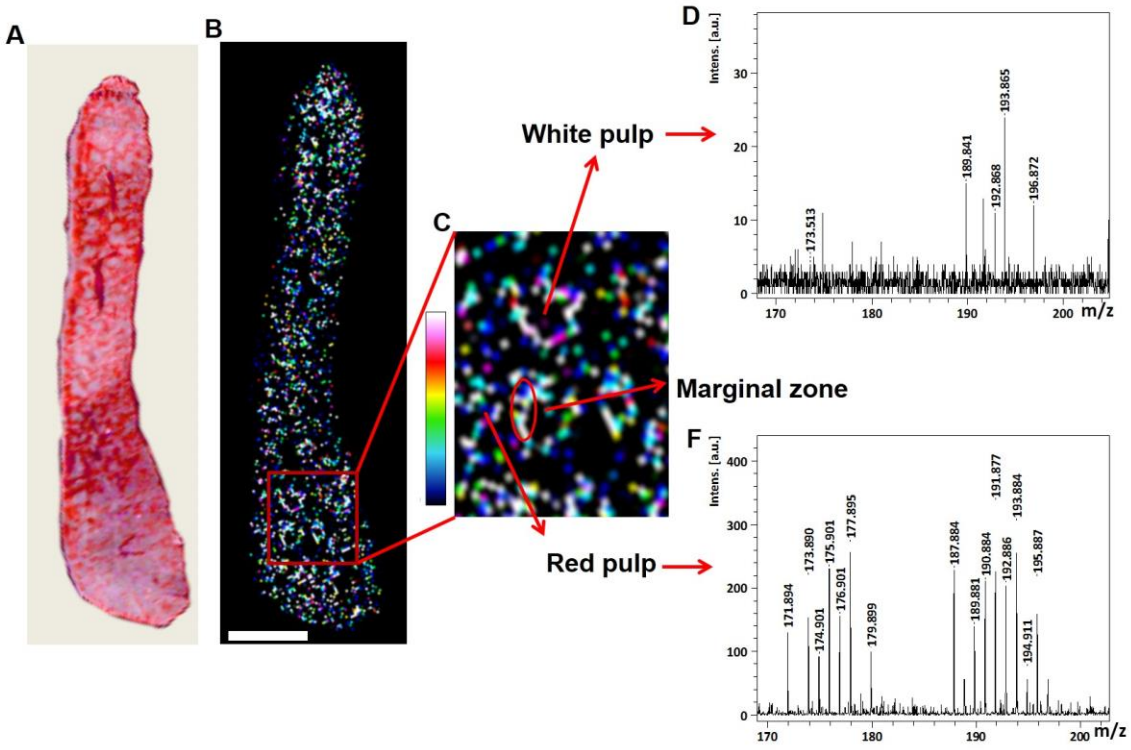

Fig. S7. Suborgan distribution of MoS_2 nanosheets in normal mouse spleen. (**A**) Optical image of spleen. (**B**) MSI image showing the sub-organ distribution of MoS_2 nanosheets. (**C**) Zoomed-in area of interest selected in B. (**D**) Representative mass spectra of white pulp. (**E**) Representative mass spectra of red pulp. The color bar indicates the intensity increase from 0 to 100% from bottom to top.

Biodistribution of MoS_2 nanosheets in subcutaneous implanted tumor model mice

Taking advantage of the unique anatomical and pathophysiological characteristic of tumor tissue, e.g., the defective architecture of the tumor blood vessel, large endothelial cell–cell gap openings (*36*, *37*) nanoparticles have been applied to passive targeting tumor tissue by the enhanced permeability and retention (EPR) effect (*38*). To better understanding how the EPR effect influence the biodistribution behavior of MoS_2 nanosheets, their biodistribution were further studied in two subcutaneous implanted tumor model: H22 tumor model and 4T1 tumor model mice. The biodistribution of bare MoS_2 nanosheets after 24 h injection in two subcutaneous implanted tumor models (fig. S9) showed MoS_2 nanosheets accumulated in lung, spleen and liver in both tumor model mice as in the normal mice, but lower accumulation of MoS_2 nanosheets are observed in both tumors. Previous studies had shown that the size, shape, surface charge of the

nanoparticles can significantly affected the kinetics and extent of tumor accumulation via EPR effect (*3*, *30*). The lower accumulation of MoS_2 nanosheets in tumors in this study may be the results of the large size of nanosheets, more than the cut-off size of the tumor vasculature pores or the complex microenvironment limits the preferential extravasation of MoS_2 nanosheets through the EPR effect (*39*). However, MoS_2 nanosheets showed slightly higher intensity in 4T1 tumor than H22 tumor, which implies the variable vasculature pore sizes and distinct microenvironment of different tumors may lead to different biodistribution behaviors of nanocarriers. In addition, the MoS_2 nanosheets showed an inhomogeneous distribution in the tumor tissues, which may relate to the inhomogeneous extravasation and delivery of nanosheets to the tumor tissue caused by heterogeneous pore sizes of the tumor vasculature (*40*). These results reminder the specific characteristics of tumor tissues should be considered in the design of nanocarriers.

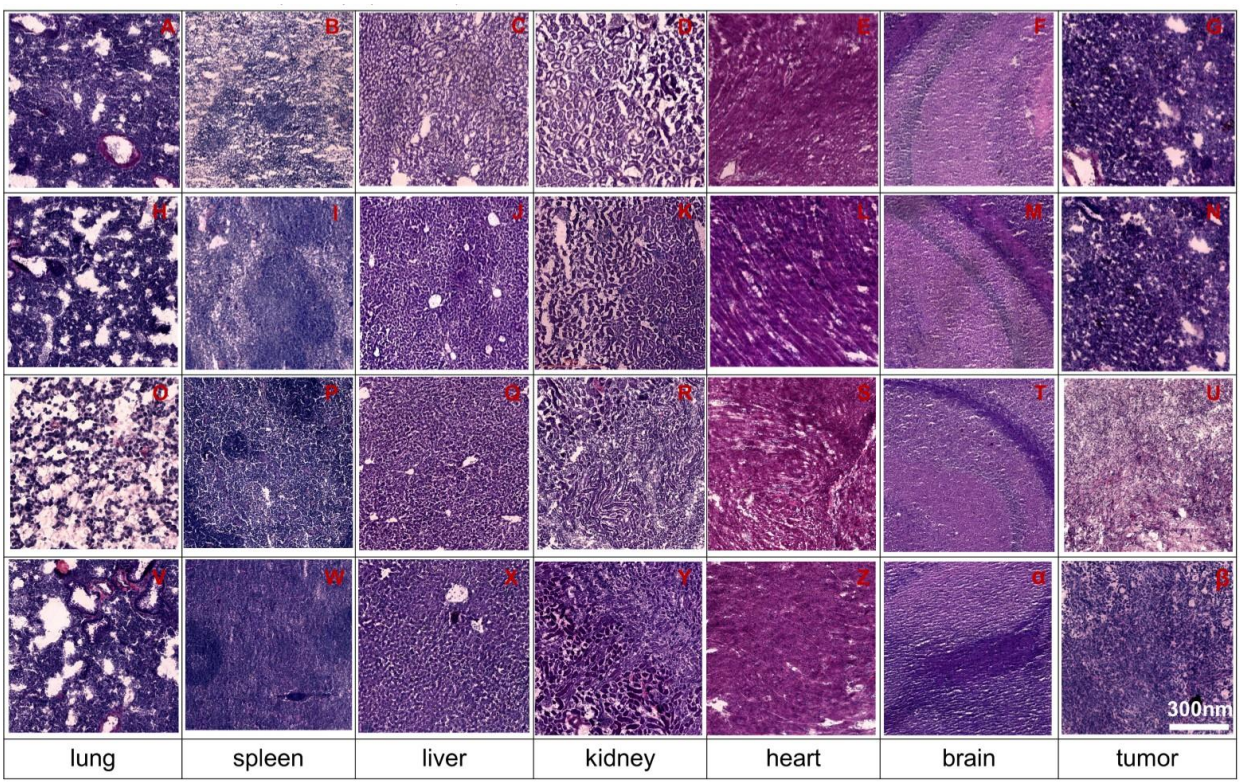

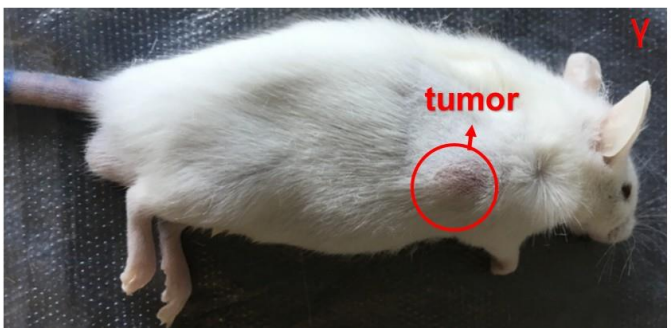

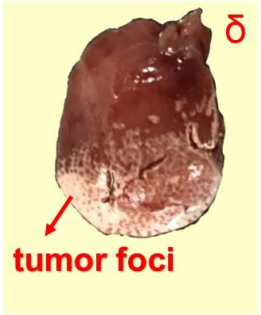

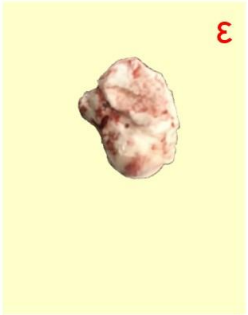

Fig. S8. H&E-stained images of tissues from the tumor model mice. (**A**)-(**G**) H&E stained images of tissues from H22 tumor model mice baring intravenous injection of bare MoS_2 nanosheets. (**H**)-(**N**) H&E stained images of tissues from H22 tumor model mice baring intravenous injection of DOX/PEG-MoS_2 nanosheets. (**O**)-(**U**) H&E stained images of tissues from 4T1 tumor model mice baring intravenous injection of bare MoS_2 nanosheets. (Y)-(β) H&E stained images of tissues from 4T1 tumor model mice baring intravenous injection of DOX/PEG-MoS_2 nanosheets. Optical images of tumor model mouse. (γ) Optical image of a mouse baring subcutaneous implanted H22 tumor. (δ) Optical image of tumor baring liver tissue. (ε) Optical image of subcutaneous implanted H22 solid tumor. All the photos in this figure was taken by Jinjuan Xue (Institute of Chemistry, Chinese Academy of Sciences).

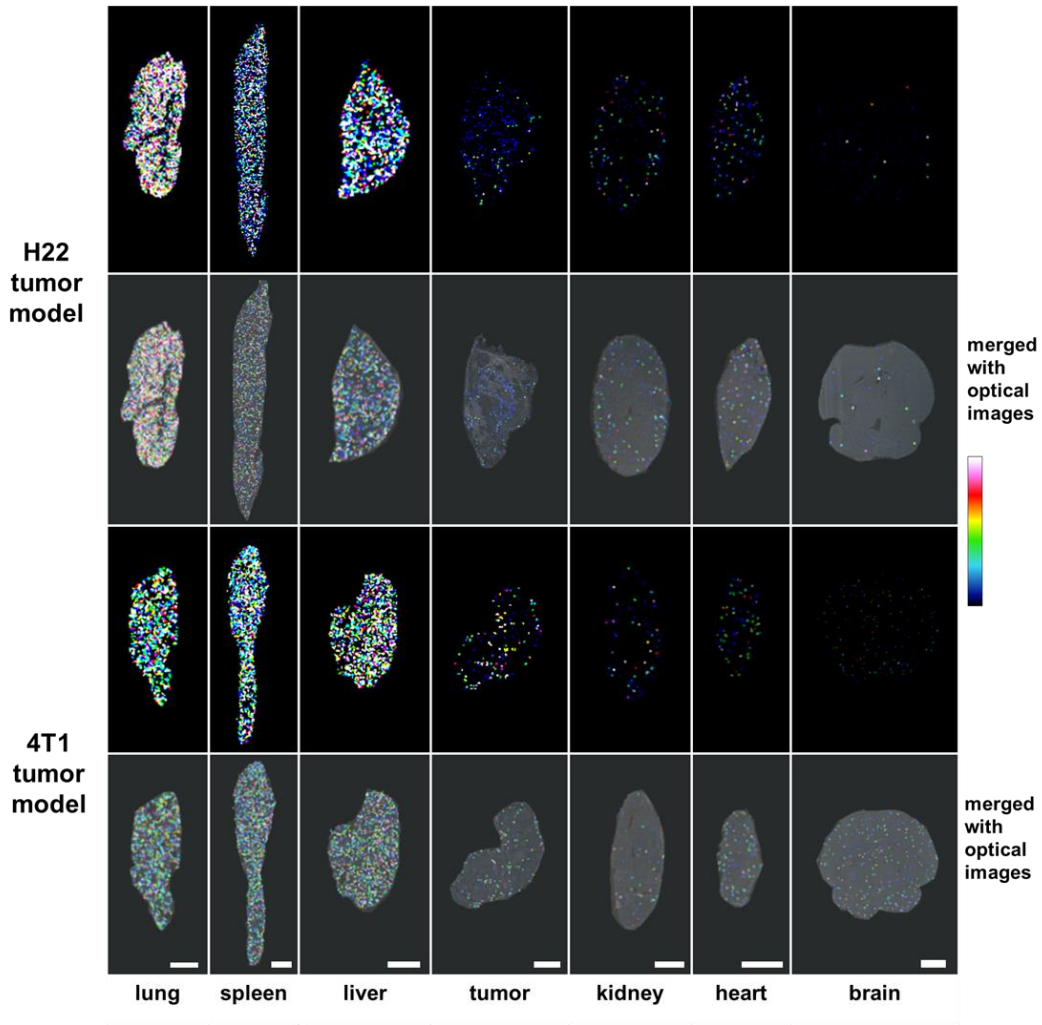

Fig. S9. LDI MSI images of tissues in subcutaneous implanted tumor models. The images show the sub-organ distribution of bare MoS_2 nanosheets after 24 h injection in H22 tumor model and 4T1 tumor model. Both of the optical images merged with LDI MSI images are shown right below the MSI image. The color bar on the right indicates the intensity increase from 0 to 100%

from bottom to top. Scale bar: 5 mm.

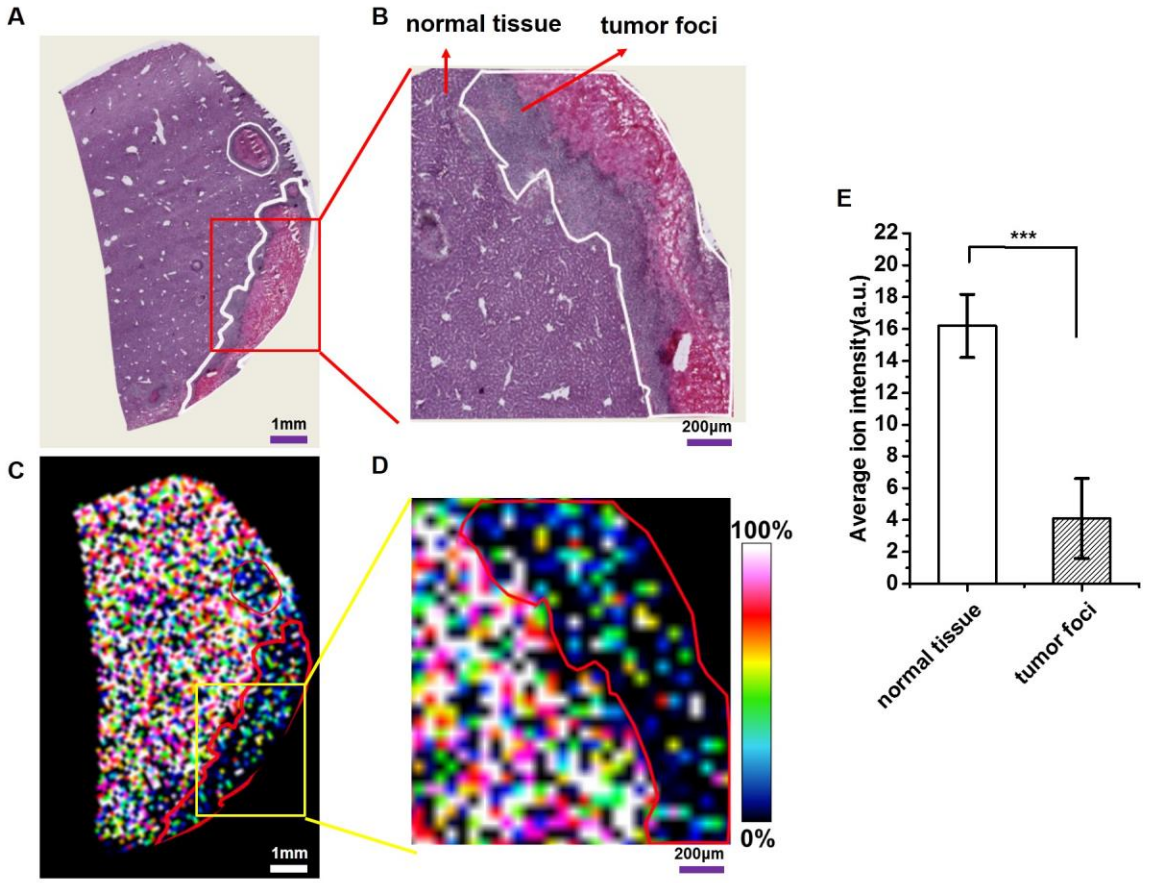

Fig. S10. Distribution of bare MoS_2 nanosheets in the liver of orthotopic H22 tumor model mice after 48-hour intravenous injection. (**A**)-(**B**) H&E stained images of the (A) tumor-baring liver tissue and (B) zoomed-in area of interest. (**C**)-(**D**) The corresponding LDI MSI image showing the distribution of bare MoS_2 nanosheets in (C) tumor-baring liver tissue and (D) the corresponding zoomed-in area. (**E**) Average ion intensity of bare MoS_2 nanosheets in normal tissue and tumor foci. Ten regions of interest (50 pixels/each) were selected in both normal tissue and tumor foci. *** $p < 0.01$. The color bar on the right indicates the intensity increase from 0 to 100% from bottom to top.

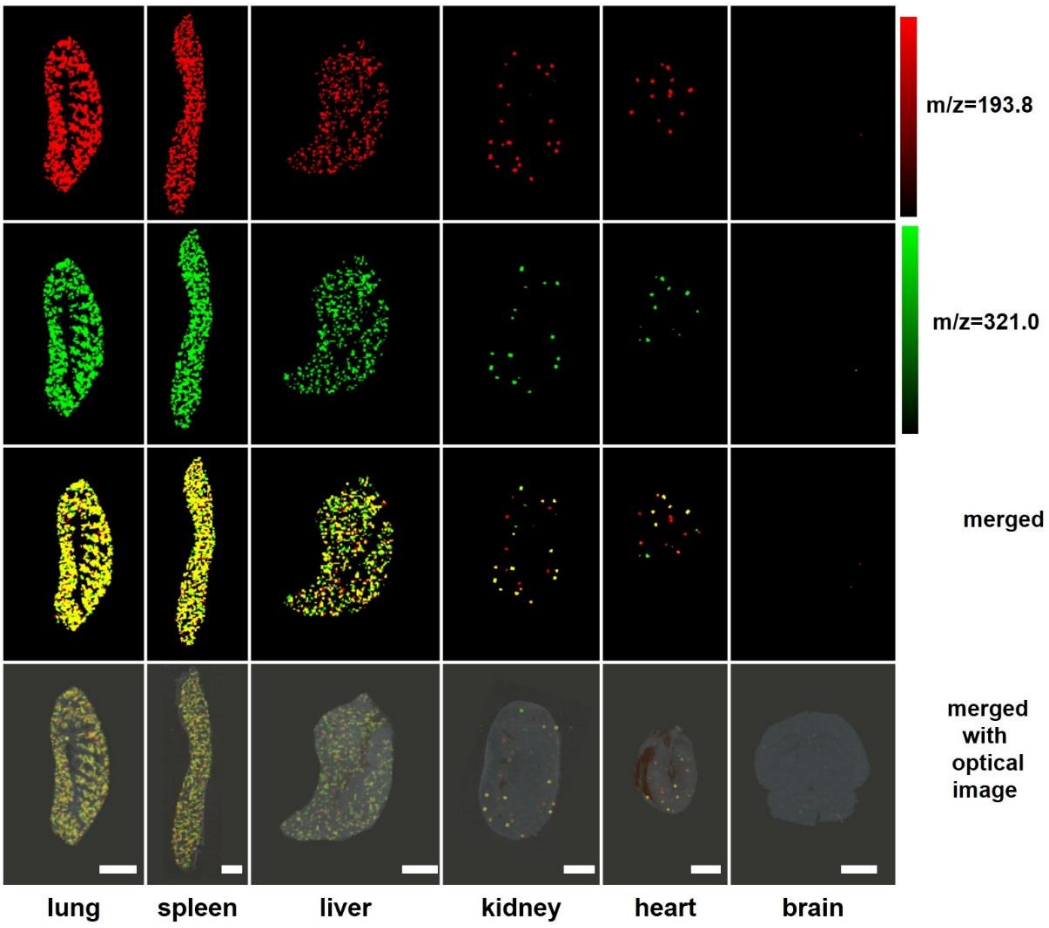

Fig. S11. LDI MSI images of MoS_2 nanosheets and their payload DOX in tissues of normal mice. The color bar on the right indicates the intensity increase from 0 to 100% from bottom to top. Scale bar: 5 mm

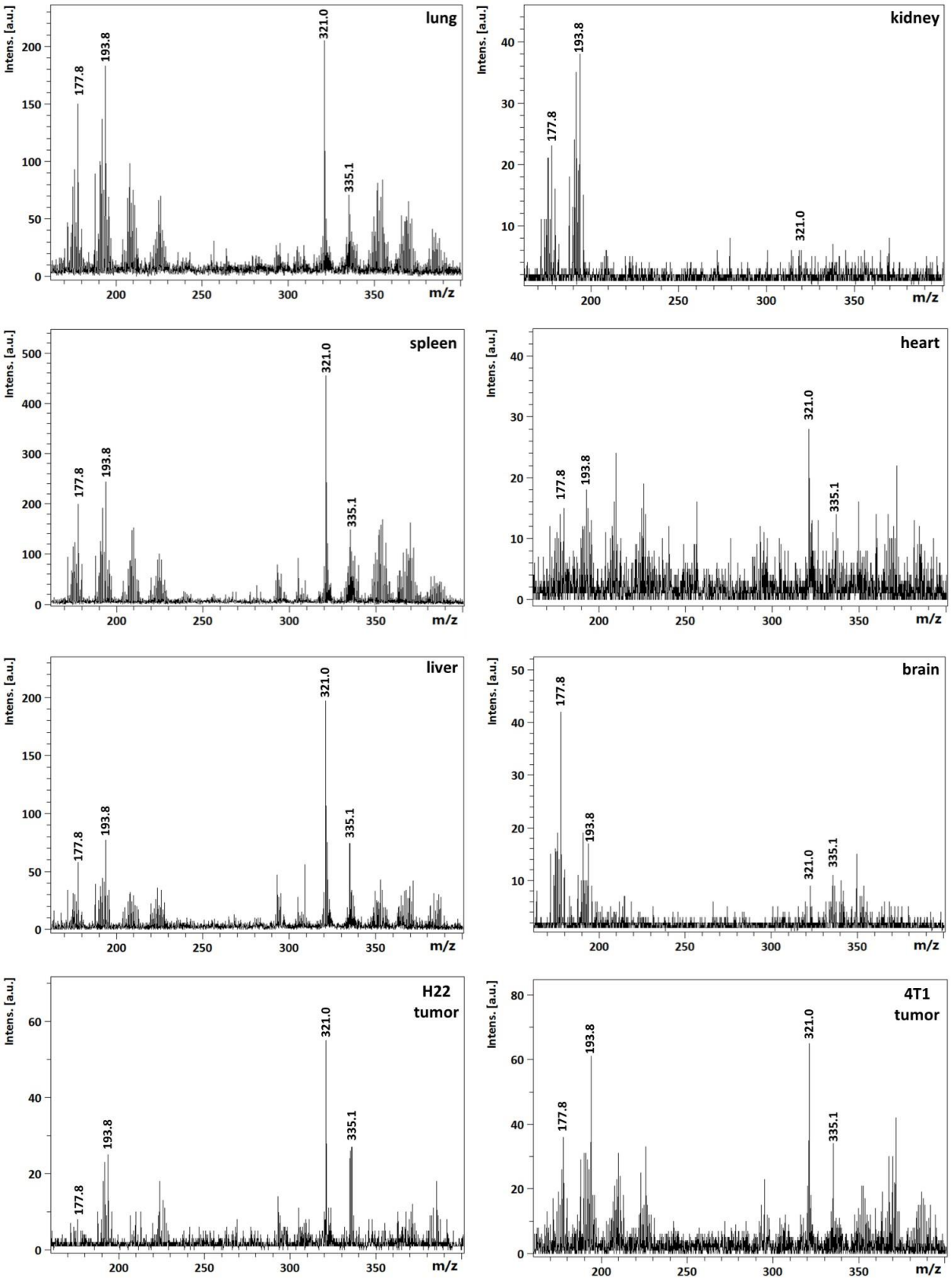

Fig. S12. Representative LDI mass spectra of DOX/PEG-MoS_2–injected mouse tissue slices. Organs harvested after 24 hours' injection, and tissues are lung, spleen, liver, kidney, heart, brain H22 tumor and 4T1 tumor.

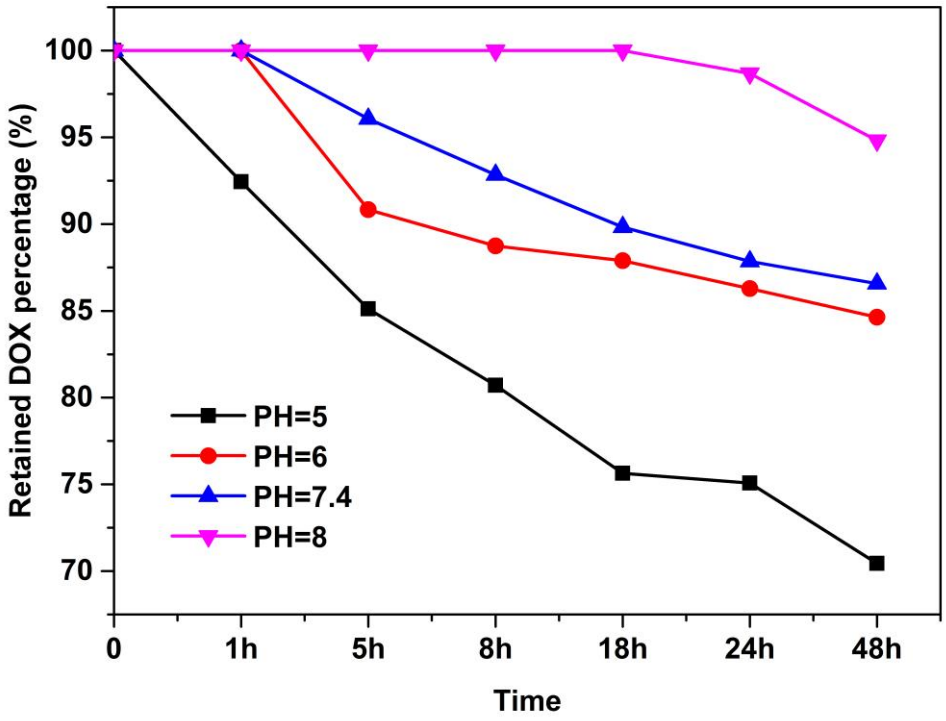

Fig. S13. Drug release from DOX/PEG-MoS_2 nanosheets at different pH values as a function of time.

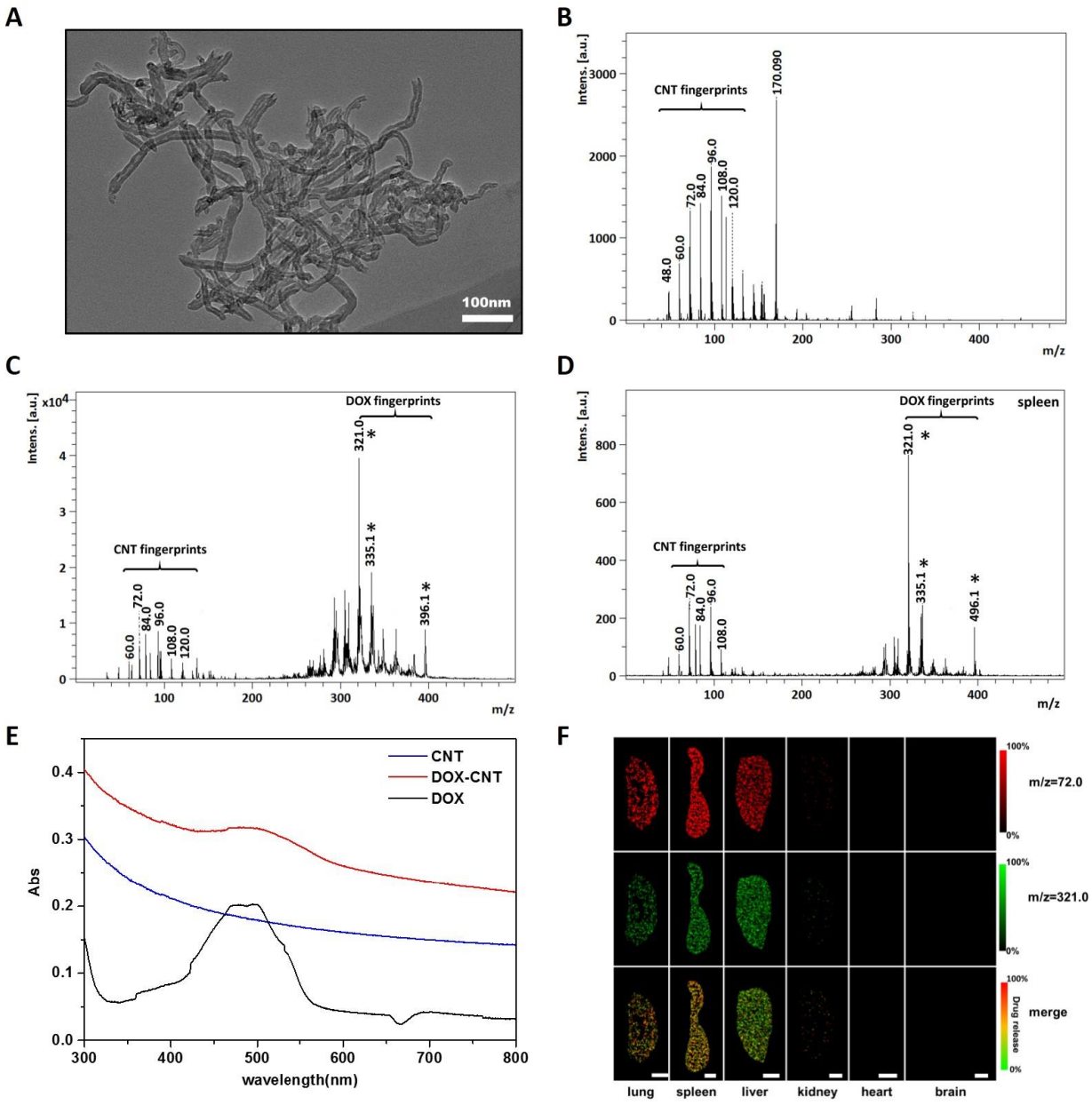

Fig. S14. LDI MSI images of CNTs (carbon nanotubes) and their payload DOX in tissues. (**A**) TEM image of oxidized CNTs. (**B**) LDI mass spectra of oxidized CNTs. (**C**) LDI mass spectra of oxidized CNTs loading with doxorubicin (DOX-CNT). (**D**) Representative LDI mass spectra of DOX-CNT injected-mice spleen tissue slice. (**E**) UV-Vis adsorption spectra of CNTs (blue line), DOX (black line) and DOX-CNT (red line). (**F**) LDI MSI images of CNTs (m/z = 72.0) and their payload DOX (m/z = 321.0) in DOX-CNT injected-mice tissues. Notes: * indicate the MS fingerprints of drug in (C) and (D).

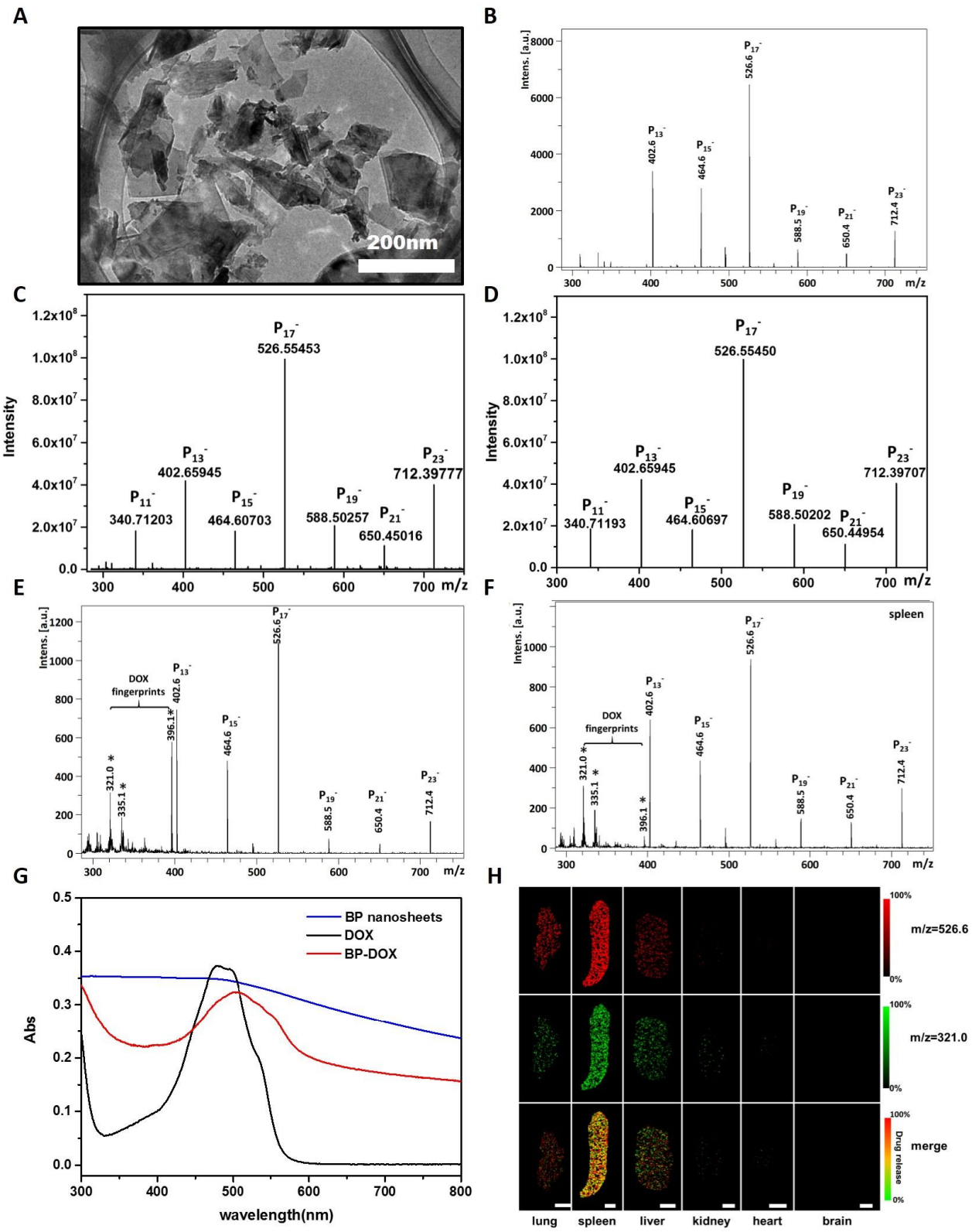

Fig. S15. LDI MSI images of black phosphorus nanosheets and their payload DOX in tissues. (**A**) TEM image of BP nanosheets. (**B**) LDI mass spectra of BP nanosheets. (**C**) High resolution LDI FT ICR mass spectra of BP nanosheets loading with doxorubicin (DOX-BP). (**D**) Theoretical BP nanosheets MS fingerprints. (**E**) Representative LDI mass spectra of DOX-BP

injected-mice spleen tissue slice. (**F**) LDI mass spectra of BP nanosheets loading with doxorubicin (DOX-BP). (**G**) UV-vis adsorption spectra of BP nanosheets (blue line), DOX (black line) and DOX-BP (red line). (**H**) LDI MSI images of BP nanosheets (m/z = 526.6) and their payload DOX (m/z = 321.0) in DOX-BP injected-mice tissues. Notes: * indicate the MS fingerprints of drug in (E) and (F).

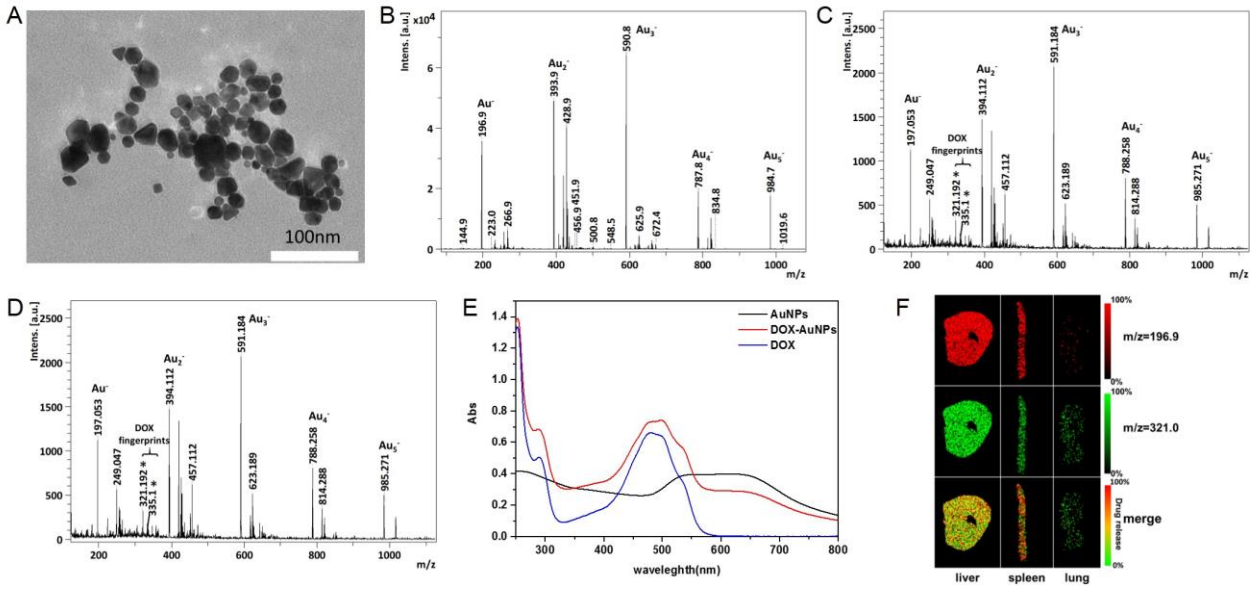

Fig. S16. LDI MSI images of gold nanoparticles and their payload DOX in tissues. (**A**) TEM image of AuNPs. (**B**) LDI mass spectra of AuNPs. (**C**) LDI mass spectra of AuNPs loading with doxorubicin (DOX-AuNPs). (**D**) Representative LDI mass spectra of DOX-AuNPs injected-mice liver tissue slice. (**E**) UV-Vis adsorption spectra of AuNPs (black line), DOX (blue line) and DOX-AuNPs (red line). (**F**) LDI MSI images of DOX-AuNPs (m/z = 196.9) and their payload DOX (m/z = 321.0) in DOX-AuNPs injected-mice tissues. Notes: * indicate the MS fingerprints of drug in (C) and (D).

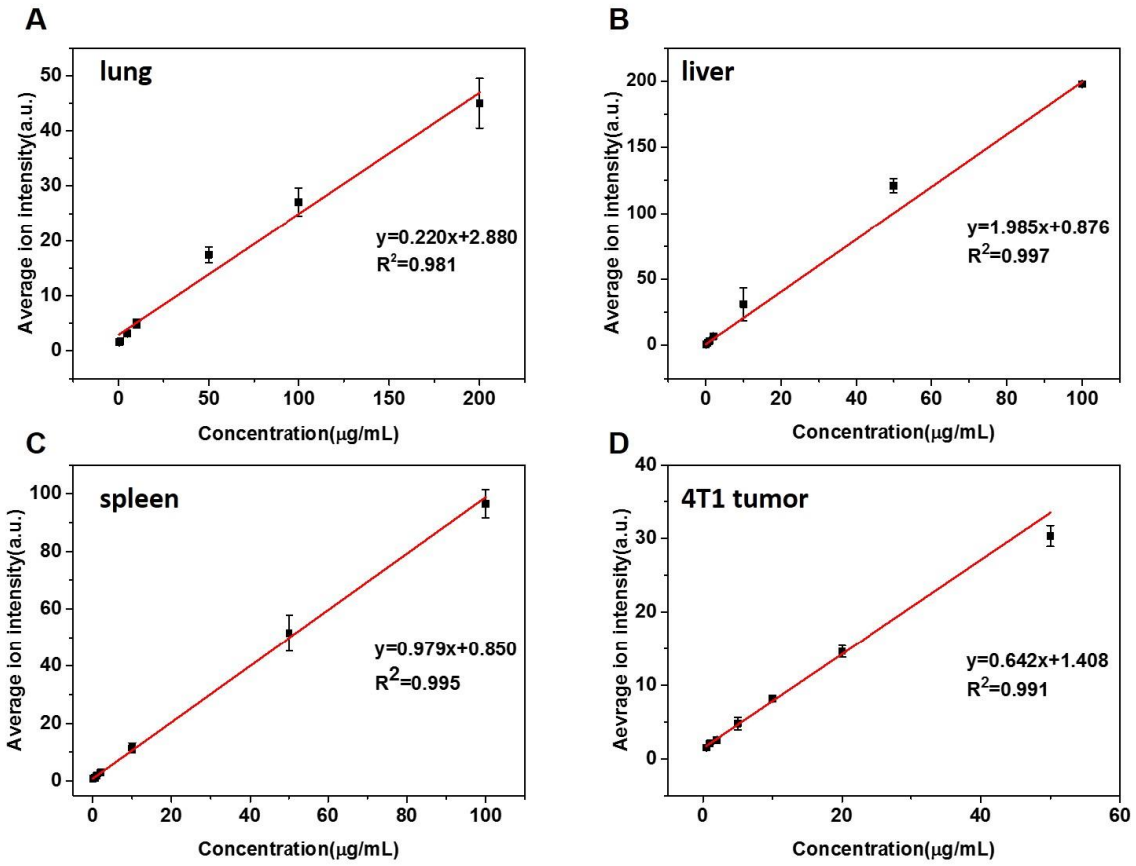

Fig. S17. Standard calibration curves for bare MoS_2 nanosheets in tissues. (**A**) lung, (**B**) liver (**C**) spleen, (**D**) 4T1 tumor.